AIAA JOURNAL
Vol. 38, No. 9, September 2000

Gross-Entrainment Behavior of Turbulent Jets Injected Obliquely into a Uniform Crossflow

Donghee Han,* V. Orozco,† and M. G. Mungal‡
Stanford University, Stanford, California 94305-3032

Turbulent jets injected at various inclinations into a uniform crossflow have been studied using Mie-scattering flow visualization and image-processing techniques. Injection angles ranging from −45 to 45 deg from the normal direction to the crossflow have been studied for the square root of momentum ratio ranging from 5 to 20. Instantaneous and ensemble-averaged images were obtained for each jet configuration, and their centerline trajectories were determined. A skewed coordinate system that accommodates changes in injection angle of the jets was used with a power-law equation to collapse the trajectories to a single profile. Combining this correlation of the jet centerline with the conservation equations of mass and momentum, an algebraic expression was derived to estimate the mass entrained by deflected jets. A jet with negative injection angles entrains the crossflow fluid more efficiently, leading to more rapid and compact mixing.

Nomenclature

A, B = trajectory constants
d = jet diameter
G = momentum ratio ($\dot{m}V/\dot{m}_j V_j$)
$\dot{m}$ = mass-flow rate
r = square root of momentum ratio $(\rho_j V_j^2/\rho_\infty V_\infty^2)^{1/2}$
s = streamline coordinate
u, v = jet velocity components in x and y direction
V = jet speed
X, Y = skewed coordinate system
x, y = orthogonal coordinate system
θ = angle with respect to normal
ρ = density

Subscripts

j = jet-exit property
∞ = crossflow property

I. Introduction

JET-IN-CROSSFLOW configurations can be found in many industrial applications, such as burner technology, chemical waste transport, and vertical/short takeoff and landing aerodynamics.[1] Often many cases arise where enhanced mixing and entrainment of fluids is sought, such as in primary combustion and in gas reburning.[2] The need to quantify the entrainment and concentration levels of the flow regime is thus essential for proper analysis and for improvement of mixing or combustion.[3] For cases where the angle of injection of a fuel or a mixing medium into a crossflow is not transverse, correlative data and analytical relations predicting the trajectory and resulting properties of the jet flow are not readily available. Platten and Keffer[4] measured the velocity field to determine the jet trajectory, but the square root of momentum ratio r was limited to eight. Expressions for these inclined jet properties could prove to be useful for manufacturing and design considerations, such as for determining an optimum angle to inject a fuel into a burner so that it entrains a maximum amount of the reactant fluid.

The trajectory for the transverse jet in crossflow has been well researched and documented[5–7] compared to jets injected at other than normal angles. They include the scalar[5,6] and velocity field measurements[7] of jet in crossflow both in nonreacting and reacting cases. Pratte and Baines[6] found that the transverse jet scales remarkably well with the length scale rd. Their analysis found that normalizing the spatial coordinates by this length scale rd enables the centerline trajectories of jets with different velocity ratios to collapse to the functional form

$$\frac{y}{rd} = A\left(\frac{x}{rd}\right)^B$$

where

$$r = \sqrt{\frac{\rho_j V_J^2}{\rho_\infty V_\infty^2}} \tag{1}$$

In Eq. (1) y is the distance from the jet exit in the original jet direction, and x is the distance in the crossflow direction. Experimental values were found for the constants A and B by different researchers, but were generally around 1.5–2.5 for A and 0.25–0.38 for B (Refs. 6–9). The difference in these values can be caused by the jet-exit profile and configurations as well as the turbulence in the crossflow and tunnel dimensions.

The same general procedure can be used to analyze deflected jet flows. Wu[10] proposed a new coordinate system that can account for the variation in injection angle and still be used with the functional form Eq. (1) by skewing the Y axis so that it is aligned with the initial jet velocity vector and aligning the X axis with the crossflow velocity vector (Fig. 1), or

$$Y = y/\cos\theta, \qquad X = x - y\tan\theta \tag{2}$$

Applying this coordinate system on data taken by Platten and Keffer,[4] Wu found that the trajectory can be collapsed to

$$Y/rd = A(X/rd)^B \tag{3}$$

This relation was derived by using the proper nondimensionalization and a momentum balance in a direction normal to the jet direction. It also assumes that the angular deviation from the normal injection θ is small, and therefore it is expected that the relation will not perform well at large inclination angles. In the present work this skewed coordinate system will be used to find the trajectory of deflected jets with various r values and injection angles, and an expression will be derived for the mass entrainment as a function of r and θ. Its limitation and application will also be discussed.

II. Experimental Methods

A. Experimental Facilities

Nonreacting turbulent air jets were discharged into a large vertical wind tunnel, and images were acquired for various injection angles and velocity ratios. The tunnel test section was rectangular in shape, 54 × 54 cm in width and 94 cm in length, and was powered by a centrifugal blower (Fig. 2a). Wire mesh and honeycomb were

Received 3 October 1998; revision received 29 August 1999; accepted for publication 18 September 1999. Copyright © 1999 by the American Institute of Aeronautics and Astronautics, Inc. All rights reserved.

*Graduate Research Assistant, Mechanical Engineering Department.
†Undergraduate Research Assistant, Mechanical Engineering Department; currently at Air Bearings Department, AlliedSignal, Inc., Torrance, CA 90504.
‡Associate Professor, Mechanical Engineering Department.

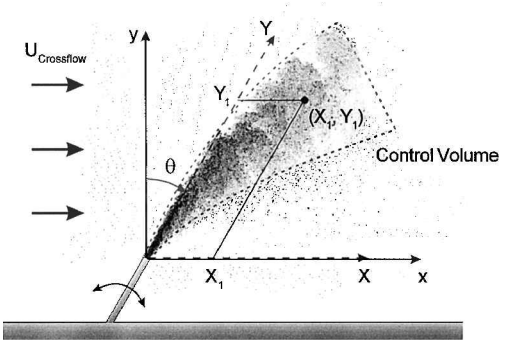

Fig. 1 Transformed coordinate system suggested by Wu[10] and control volume used for entrainment analysis.

located at the inlet of the tunnel to ensure a uniform velocity profile throughout the test section. Further details of the tunnel facility can be found in Smith.[11] The jets were introduced to the flow by a $\frac{1}{4}$-in. (6.35-mm) tubing with inner diameter of 4.6 mm inserted through the center of a removable aluminum disk. Disks were made for injection angles of ±15, ±30, and ±45 deg, where 0 deg is the transverse case. The jet-exit tubing extended into the tunnel so that it discharged outside the natural boundary layer. Thin cross-shaped plates, each about an inch long, were inserted inside the tube more than 50 jet diameters upstream of jet exit to eliminate the swirl of the exit flow after the bend in the flexible tubing. The air supply for the jet was monitored and controlled with a flow meter (Matheson Model 605) and pressure gauge (Norgren; 0–30-psi range), enabling flow rates to be easily set. The tunnel speed was set by adjusting

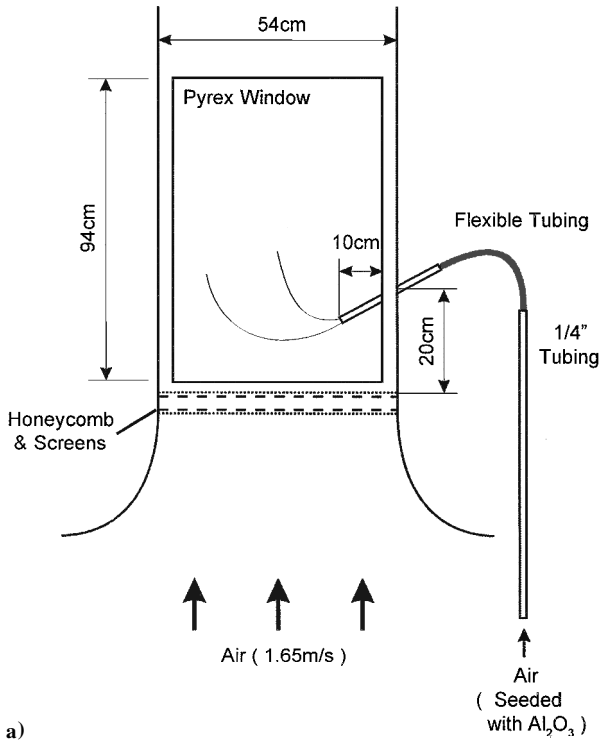

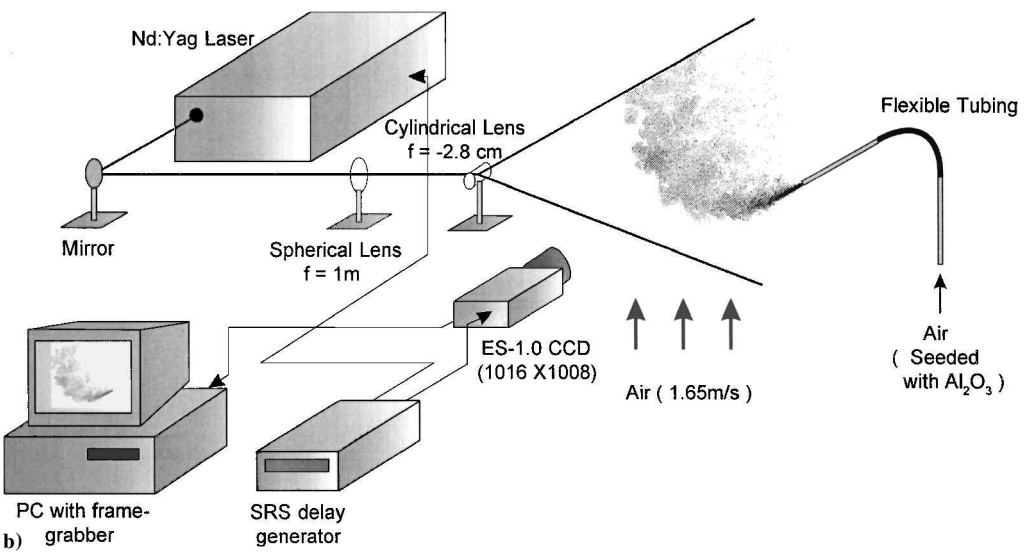

Fig. 2 Experimental setup showing the a) tunnel facility and b) Mie-scattering arrangement.

the air damper far downstream of the test section, and the speed was measured using PIV technique. The square roots of momentum ratio, which is simply the velocity ratio in this case, tested for each injection angle were 5, 10, and 20, corresponding to Reynolds numbers of 2.6×10^3, 5.2×10^3, and 10.4×10^3, respectively.

Image data acquisition was made possible using Mie-scattering flow visualization with alumina (Al_2O_3, 0.1-μm nominal diameter) particle seeding of the jets (Fig. 2b). Particles along the center plane of the jets were illuminated with a 250-μm thick laser sheet from a pulsed second harmonic of Nd:YAG laser with a pulse width of 10 ns, pulse energy of 250 mJ, operating at 532 nm. Planar side-view images of the jets were acquired using a nonintensified charge-coupled device array (Kodak ES-1.0) with 1016×1008 pixel resolution. Timing of the camera with the laser was controlled with a four-channel digital delay/pulse generator (Stanford Research Systems DG-535), and output digital images were sent to a computer via an AIA interface connector and frame grabber board. One-hundred instantaneous images were acquired for each jet configuration at 7.35 frames per second, and an image-processing software (MATLAB®) was used later to obtain time-averaged profiles for each ensemble. Each image was subtracted by the background, but was not corrected for the laser sheet profile.

B. Experimental Uncertainties

Uncertainties in experiment can be summarized as 1) uncertainties induced by the facility itself and 2) uncertainties in determining the trajectory. First, the freestream velocity of the tunnel has about 5% maximum-to-minimum nonuniformity, which can lead to about 5% relative uncertainty in r value. Also, the extended tube can cause vortex shedding, which might affect the wake structure of the jet; however, Su and Mungal[12] reported that the trajectory of a transverse jet with $r = 5$ was minimally affected by the extended tube and its vortex structure. From the similarity analysis given by Hasselbrink,[7] it is evident that the influence of the extended tube will be less for higher r values. Therefore, we can neglect the influence of the extended tube for the purpose of trajectory determination.

Each pixel of the camera represented approximately a 300×300 μm region, and because the scale of the jet trajectory is always larger than the jet diameter (4.6 mm), the resolution was sufficient to determine the trajectory from the image. Jet direction was determined using a smooth curve (Bezier) on the averaged image represented with color contours, and the maximum concentration point was determined normal to this jet direction. It is possible that the jet direction determined by this method can be different from that determined by the velocity field and most likely is based on

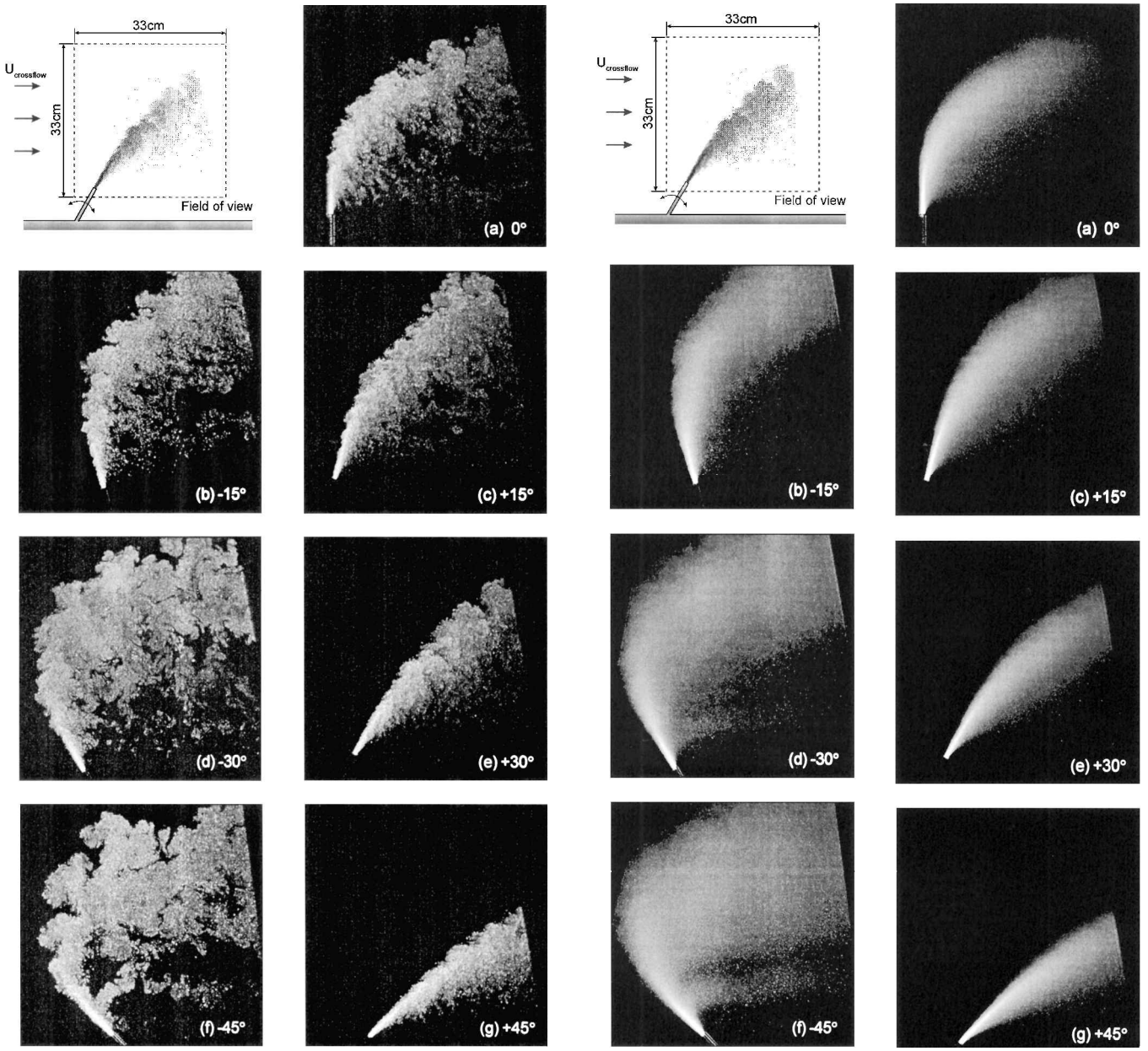

Fig. 3 Instantaneous images for $r = 20$ jets: $Re = 10.4 \times 10^3$, u_{jet} = 33 m/s, and $u_{crossflow}$ = 1.65 m/s.

Fig. 4 Time-averaged images for $r = 20$ jets: $Re = 10.4 \times 10^3$, u_{jet} = 33 m/s, and $u_{crossflow}$ = 1.65 m/s.

the results of Ref. 7. Finally, the correlation coefficients of the least-square fittings were higher that 0.95 for all of the r values examined.

III. Results and Discussion

A. Jet Structure

Sample instantaneous images for the $r = 20$ jets are shown in Fig. 3, and the corresponding ensemble-averaged images are shown in Fig. 4. Figures 5 and 6 show the instantaneous and ensemble-averaged images for the $r = 10$ and 5 jets. General characteristics of the jet structures can be observed. The negative-angled jets are larger in size compared to the positive angled jets, increasing in width as the jets are angled further into the crossflow. Along with this increase in dimensions, the gradual development of a wake structure issuing from the jet exit is observed. In Fig. 3 the wake is noticeable at an injection angle of -30 deg (Fig. 3d) and becomes larger and more clearly defined at -45 deg (Fig. 3f). This formation is also observed for the $r = 10$ case at -45 deg but not as distinctly at an angle of -30 deg. Therefore, it is suspected that this formation could be dependent on not only r value, but on the angle of injection θ as well. Smith and Mungal[5] found that the progression of jet fluid in the wake structure is r dependent for the transverse jet ($\theta = 0$ deg) with a uniform jet velocity profile.

Comparing the jets with different velocity ratios, we can observe the large difference in the penetration depth of the jet fluid into the crossflow. Especially for the $r = 5$ jets injected at negative angles (Figs. 5b and 6b), the jet turns immediately after a short potential core region, and its structure does not develop significantly more than positively oriented or vertical jets, which is contrary to the $r = 10$, 20 cases. The additional differences between the $r = 5$ case and the $r = 10$, 20 cases will be discussed later.

In the present work a significant and immediate escape of the jet fluid into the wake structure is observed for jets injected at negative angles. This may be attributed to the experimental setup that uses a long extruded tube, instead of a flush convergent nozzle. Thus, the jet-exit velocity profile, which will be a fully developed pipe flow distorted by the crossflow, will likely contain portions where the momentum is not high enough to penetrate the crossflow. Other reasons for the origin of the jet fluid in the wake structure is discussed in Smith and Mungal[5] and are based on the jet/wake vorticity dynamics; such factors may also be at play in the results presented here.

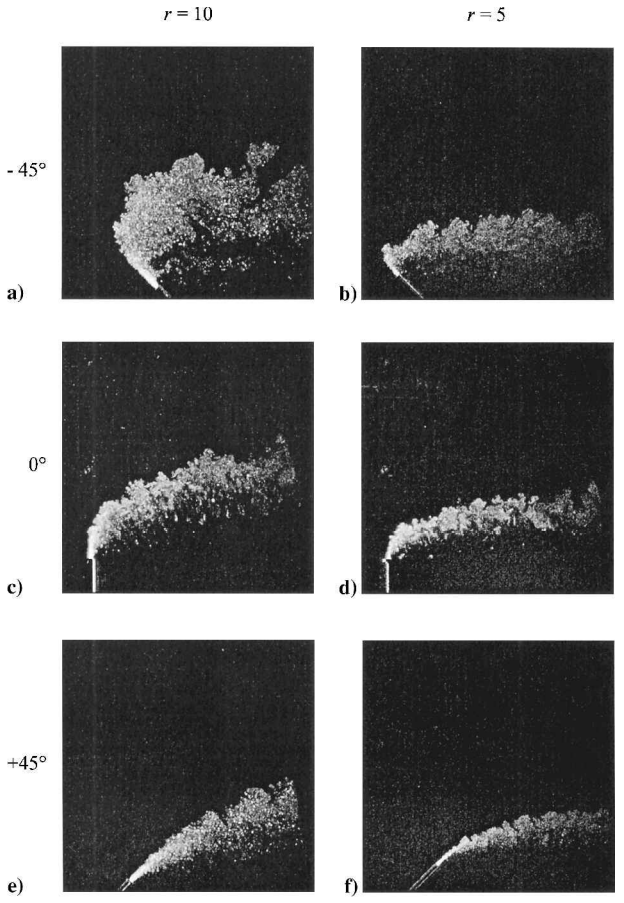

Fig. 5 Instantaneous images for $r = 10$ and 5 jets: a), c), and e) for $r = 10$, $Re = 5.2 \times 10^3$, $u_{jet} = 16.5$ m/s, and $u_{crossflow} = 1.65$ m/s; b), d), and f) for $r = 5$, $Re = 2.6 \times 10^3$, $u_{jet} = 8.25$ m/s, and $u_{crossflow} = 1.65$ m/s.

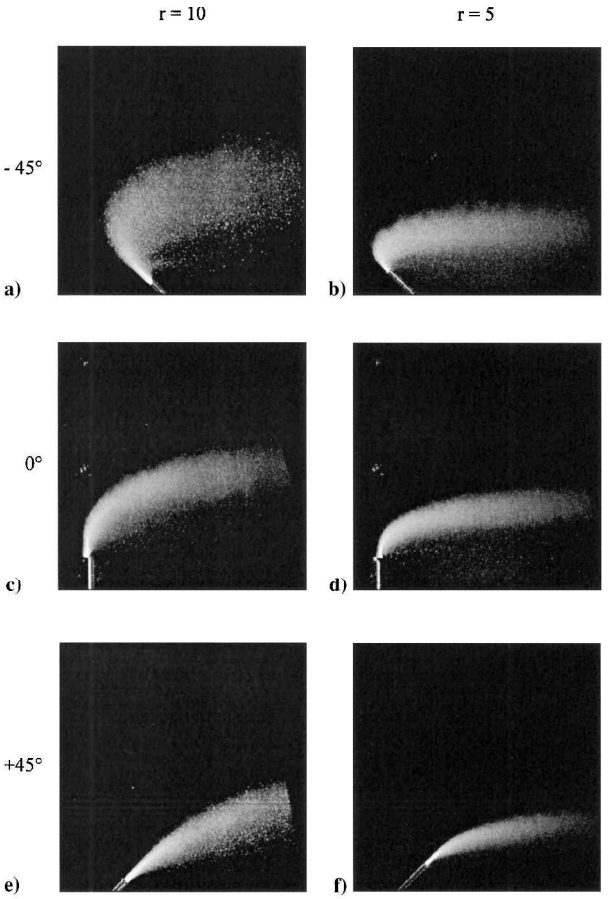

Fig. 6 Time-averaged images for $r = 10$ and 5 jets: a), c), and e) for $r = 10$, $Re = 5.2 \times 10^3$, $u_{jet} = 16.5$ m/s, and $u_{crossflow} = 1.65$ m/s; b), d), and f) for $r = 5$, $Re = 2.6 \times 10^3$, $u_{jet} = 8.25$ m/s, and $u_{crossflow} = 1.65$ m/s.

B. Jet Trajectory

The definition for the jet trajectory used in this paper is the same as that used by Smith and Mungal[5] as the locus of points in the center plane where the maximum mean concentration value occurs in a line perpendicular to the local jet direction. This trajectory can be different from the trajectory obtained by maximum local velocity.[13,14]

Trajectories for the three velocity ratios studied are plotted in Fig. 7. Trajectories are estimated by tracing the centerline path on color contour plots of each ensemble-averaged jet image. The x and y coordinates for each plot are normalized by the length scale rd and are shown in a frame $3rd$ wide and $3.5rd$ high. The $r = 10$ and 20 jets appear to be quite similar when plotted with this length scale, suggesting that these deflected jets can be scaled with rd like the transverse jet. The $r = 5$ case does not seem to scale with the $r = 10$ and 20 jets, as has also been found to be the case by Smith and Mungal.[5]

The correlation for centerline trajectories was found using linear regression in log space and is plotted in the coordinate system proposed by Wu[10] in Fig. 8, for all of the velocity ratios and injection angles. The coefficients of Eq. (3) obtained from linear regression are $A = 2.1$ and $B = 0.29$ with a correlation coefficient of least-square fitting of 0.953. These values are somewhat different from the result of Wu,[10] who obtained $A = 1.75$ and $B = 0.38$ by analyzing the experimental data of Platten and Keffer.[4] These differences can be attributed partly to differences in the experimental setup and partly to the measurement method. The jet used by Platten and Keffer[4]

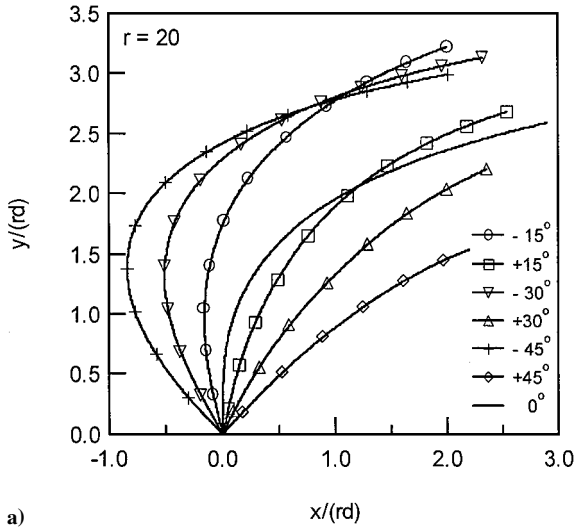

a)

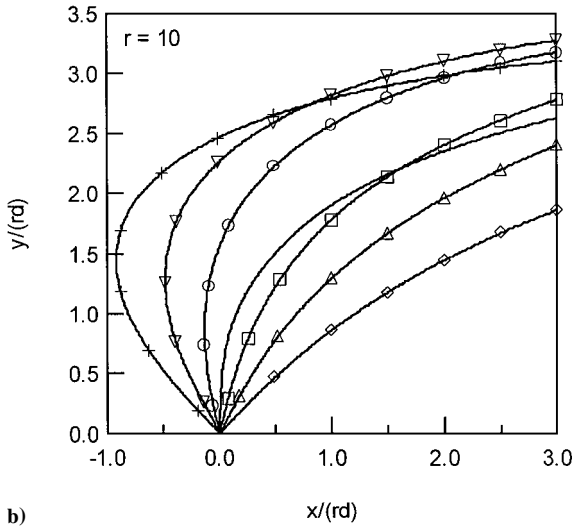

b)

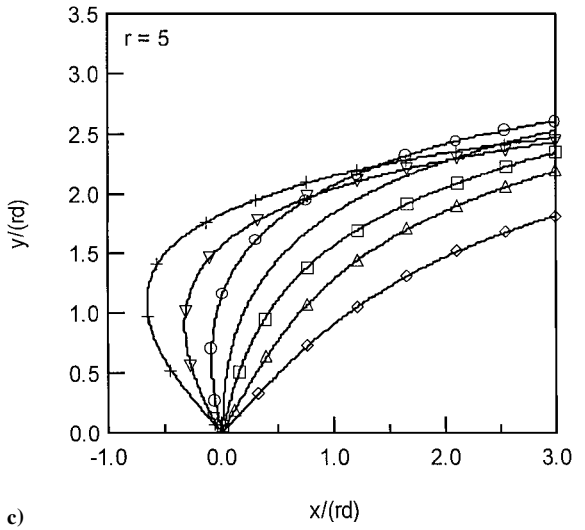

c)

Fig. 7 Centerline trajectories of deflected turbulent jets in *rd* space.

originated from a nozzle flush with a false inner wall, whereas the jet used here is injected from a tube extended out from the wall. Furthermore, in experimental approach the scalar field was measured in this work, and the velocity field was measured by Platten and Keffer.[4]

C. Discussion

Figures 9a–9c show separate plots for the different velocity ratios in order to highlight their differences. Compared to the $r = 10$, 20

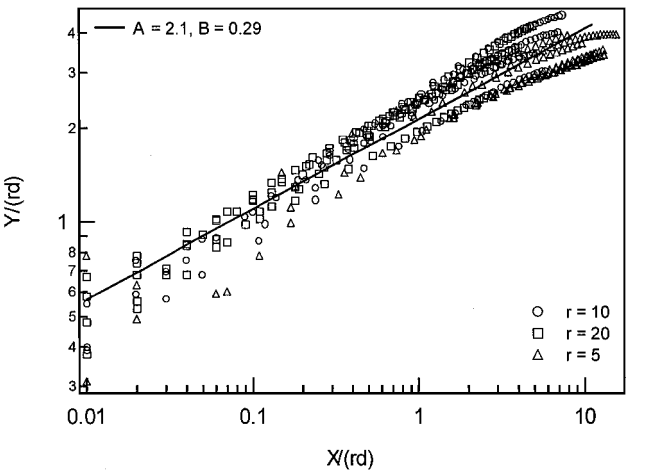

Fig. 8 Correlation of trajectory data for all of the injection angles and velocity ratios in $X/(rd)$–$Y/(rd)$ coordinates.

cases, the $r = 5$ case seems to have a higher exponent at the near field and asymptotes to a lower exponent ($B \sim 0.2$) in the far field. Smith and Mungal[4] have suggested that the presence of a low-pressure region located behind the jet exit influences the trajectory at lower velocity ratios, as well as interaction of the jet with the boundary layer of the wall. In addition, the jet Reynolds number for the $r = 5$ case is only 2.6×10^3 so that the turbulence may be insufficiently developed compared to the other cases. It is possible that these factors played a role in the current investigation, but it may also be that the $r = 5$ jet is simply a fundamentally different flow regime and should be classified separately, as suggested by Smith and Mungal.[4]

Finally, we note that the coordinate transformation proposed by Wu[10] uses the approximation that $\cos\theta \sim 1$ to eliminate θ from the correlation, which of course is only valid for small θ. This limitation is apparent from the scatter of the data for different deflection angles as shown in Figs. 7a–7c. This scatter is most noticeable for the $r = 5$ case and large deflection angles.

D. Mass Entrainment

Using the centerline trajectory information, Hasselbrink and Mungal[15] were able to derive a correlation to estimate the mass entrained by the transverse jet, as well as the mean scalar concentration and the velocity along the centerline, with good agreement to experimental data. Their analysis is based on the fact that the entrainment is the main mechanism that leads to the deflection of turbulent jet compared to pressure drag mechanism.[16] In the analysis the entrainment was estimated by calculating the momentum of the crossflow fluid required to turn the flow to the experimentally determined trajectory and gave the following expression for the mass entrainment:

$$\frac{\dot{m}}{\dot{m}_j} = 1 + \frac{r}{AB}\sqrt{\frac{\rho_\infty}{\rho_j}}\left(\frac{x}{rd}\right)^{1-B} \tag{4}$$

Here the mass-flow rate $\dot{m}$ is the sum of the initial jet mass-flow rate $\dot{m}_j$ and the mass-flow rate entrained from the crossflow stream $\dot{m}_e$.

Applying the same analysis as Ref. 15, the entrainment rate for deflected jets is similarly obtained. Mass and momentum conservation equations in Eqs. (5) have to be solved for the control volume containing the jet, as shown in Fig. 1.

Mass:

$$\dot{m} = \dot{m}_j + \dot{m}_e \tag{5a}$$

x momentum:

$$\dot{m}_j V_j \sin\theta + \dot{m}_e V_\infty = \dot{m}u \tag{5b}$$

y momentum:

$$\dot{m}_j V_j \cos\theta = \dot{m}v \tag{5c}$$

The resulting relation for the entrainment is given as

$$\frac{\dot{m}}{\dot{m}_j} = 1 + \frac{V_j}{V_\infty}\left(\frac{\mathrm{d}x}{\mathrm{d}y}\cos\theta - \sin\theta\right) \tag{6}$$

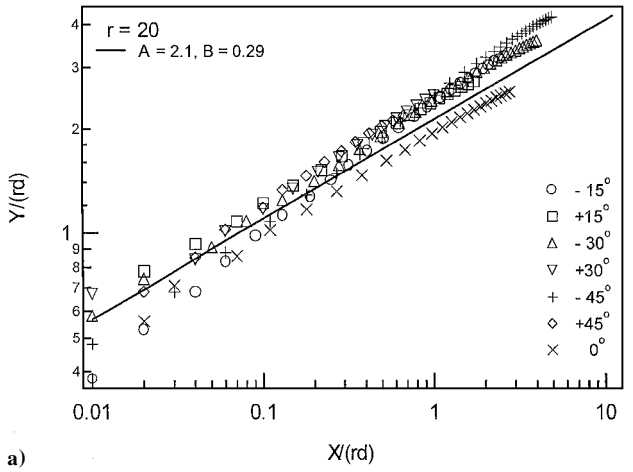

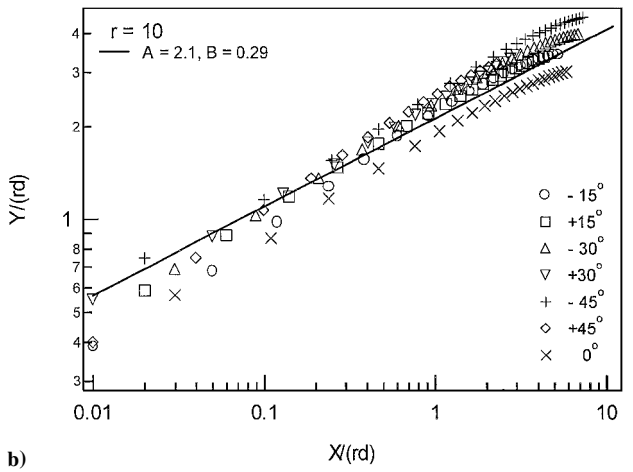

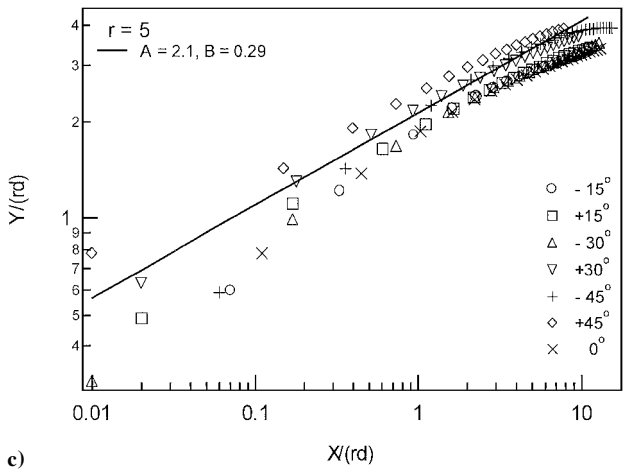

Fig. 9 Correlation of trajectory data for different injection angles and velocity ratios in *X*/(*rd*)–*Y*/(*rd*) coordinates.

The slope (dx/dy) in Eq. (6) can be obtained by differentiating Eq. (3) with the relations (2) in it. The momentum ratio ($G = \dot{m}V/\dot{m}_j V_j$) also can be derived as

$$G = \frac{ds}{dy}\cos\theta \tag{7}$$

Figure 10a shows the resulting entrainment along the jet centerline for jets injected at various angles. Apparently, jets injected at negative angles have higher entrainment, which can be expected from the large spreading rate along the centerline shown in the averaged images. Figure 10b shows the entrainment along the x direction. The observation can be made that the jet oriented upstream is a faster and more compact mixer in the crossflow direction when compared to normally injected transverse jets. This can also be observed in the instantaneous jet structures shown in Fig. 3. As the jet injection angle varies from positive to negative values, we can observe the increasing engulfing motion caused by the large structure along the windward side of the jet, which implies higher entrainment. Therefore, when the jet is used to mix fluids in a confined crossflow environment, such as gaseous fuel injection in a burner, the jet oriented upstream will significantly enhance the mixing efficiency. Applications of these ideas, as related to NO_X predictions in boiler flows, can be found in Ref. 17.

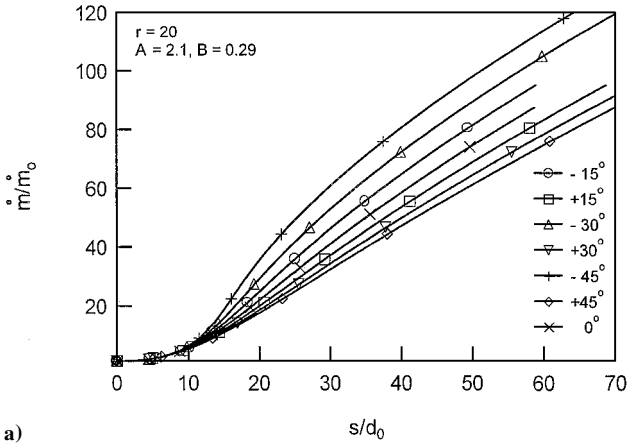

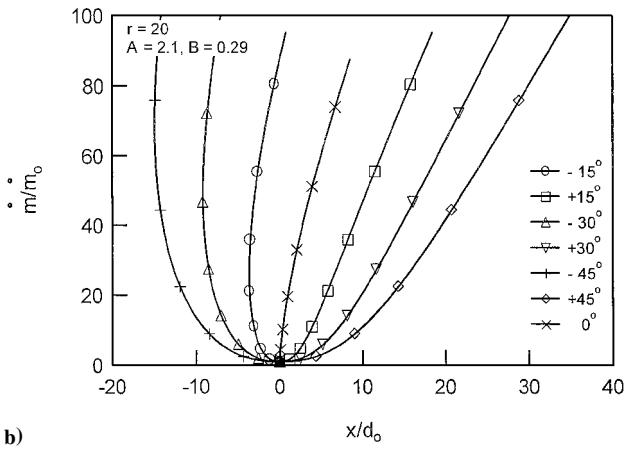

Fig. 10 Mass entrainment along the a) centerline of the jet and b) crossflow direction.

Finally, the present study has dealt with the single unconfined jet with oblique injection. For transverse injection confinement effects and the effects of multiple jets can be found in Ref. 18, but we are unaware of similar results for obliquely injected jets.

IV. Conclusions

In this study the trajectory of obliquely injected jets is determined using Mie-scattering. A coordinate transformation is used to correlate the trajectory data to a simple power law with a good agreement for $r = 10$ and 20 jets and lesser agreement for $r = 5$. From the determined trajectory the entrainment rate can be estimated using mass and momentum conservation equations.

Observation of the instantaneous and averaged images shows a distinctly higher spreading rate for jets injected at negative angles. Also, immediate escape of the jet fluid into the wake region is clearly observed, which may be attributed to the low momentum fluid caused by using a long, extruded tube configuration instead of a flush convergent jet.

Acknowledgments

This work is sponsored by the Gas Research Institute, with R. V. Serauskas as technical monitor. The authors gratefully acknowledge valuable discussions with L. Su. V. Orozco was supported by the Stanford Summer Undergraduate Research Fellowship program, and D. Han is supported by the Stanford Graduate

Fellowship program (Mr. and Mrs. Benhamou Fellow). The detailed comments provided by the reviewers are appreciated.

References

[1]Margason, R. J., "Fifty Years of Jet in Crossflow Research," *Conference on Computational and Experimental Assessment of Jet in Crossflow*, AGARD, CP-534, 1993.

[2]Zamansky, V. M., Maly, P. M., and Ho, L., "Family of Advanced Reburning Technologies: Pilot Scale Development," *Proceedings of the 1997 ASME International Joint Power Generation Conference*, 1997.

[3]Broadwell, J. E., and Lutz, A. E., "A Turbulent Jet Chemical Reaction Model: NO_X Production in Jet Flames," *Combustion and Flame*, Vol. 114, No. 3/4, 1998, pp. 319–335.

[4]Platten, J. L., and Keffer, J. F., "Deflected Turbulent Jet Flows," *Journal of Applied Mechanics*, Vol. 38, No. 4, 1971, pp. 756–758.

[5]Smith, S. H., and Mungal, M. G., "Mixing, Structure and Scaling of the Jet in Crossflow," *Journal of Fluid Mechanics*, Vol. 357, 1998, pp. 83–122.

[6]Pratte, B. D., and Baines, W. D., "Profiles of Round Turbulent Jet in a Crossflow," *Journal of Hydronautics*, Vol. 92, 1967, pp. 53–64.

[7]Hasselbrink, E. F., "Transverse Jets and Jet Flames: Structure, Scaling, and Effects of Heat Release," Ph.D. Dissertation, Mechanical Engineering Dept., HTGL Rept. TSD-121, Stanford Univ., Stanford, CA, July 1999.

[8]Margason, R. J., "The Path of a Jet Directed at Large Angles to a Subsonic Free Stream," NASA TN D-4919, 1968.

[9]Storm, K. R., "Low-Speed Wind Tunnel Investigation of a Jet Directed Normal to the Wind," Aeronautics Lab., Rept. 885, Univ. of Washington, Seattle, WA, 1965.

[10]Wu, J., "Near-Field Trajectory of Turbulent Jets Discharged at Various Inclinations into a Uniform Crossflow," *AIAA Journal*, Vol. 11, No. 11, 1973, pp. 1579–1581.

[11]Smith, S. H., "The Scalar Concentration Field of the Axisymmetric Jet in Crossflow," Ph.D. Dissertation, Mechanical Engineering Dept., HTGL Rept. T-328, Stanford Univ., Stanford, CA, Aug. 1996.

[12]Su, L. K., and Mungal, M. G., "Simultaneous PIV/PLIF Measurements in Turbulent Crossflowing Jets with Low Velocity Ratio," *Proceedings of the Third International Workshop on PIV '99*, 1999, pp. 333–338.

[13]Kamotani, Y., and Greber, I., "Experiments on a Turbulent Jet in a Crossflow," *AIAA Journal*, Vol. 10, No. 11, 1972, pp. 1425–1429.

[14]Haniu, H., and Ramaprian, B. R., "Studies on Two-Dimensional Curved Non-Buoyant Jets in Crossflow," *Journal of Fluids Engineering*, Vol. 111, No. 1, 1989, pp. 78–86.

[15]Hasselbrink, E. F., and Mungal, M. G., "An Analysis of the Time-Averaged Properties of the Far Field of the Transverse Jet," AIAA Paper 96-0201, Jan. 1996.

[16]Coelho, S. L. V., and Hunt, J. C. R., "The Dynamics of the Near Field of Strong Jets in Crossflows," *Journal of Fluid Mechanics*, Vol. 200, 1989, pp. 95–120.

[17]Han, D., Mungal, M. G., Zamansky, V. M., and Tyson, T. J., "Prediction of NO_X Control by Basic and Advanced Gas Reburning Using the Two-Stage Lagrangian Model," *Combustion and Flame*, Vol. 119, No. 4, 1999, pp. 483–493.

[18]Holdeman, J. D., "Mixing of Multiple Jets with a Confined Subsonic Crossflow," *Progress in Energy and Combustion Science*, Vol. 19, 1993, pp. 31–70.

P. R. Bandyopadhyay
Associate Editor